PCCP

PAPER

View Article Online
View Journal | View Issue

Cite this: *Phys. Chem. Chem. Phys.*, 2015, **17**, 11593

Large piezoelectric response of $BiFeO_3/BaTiO_3$ polycrystalline films induced by the low-symmetry phase

Y. F. Hou,[a] W. L. Li,[ab] T. D. Zhang,[a] W. Wang,[a] W. P. Cao,[a] X. L. Liu[c] and W. D. Fei*[a]

Received 6th March 2015,
Accepted 27th March 2015

DOI: 10.1039/c5cp01320h

www.rsc.org/pccp

$BaTiO_3$, $BiFeO_3$ and $BiFeO_3/BaTiO_3$ polycrystalline films were prepared by the radio frequency magnetron sputtering on the $Pt/Ti/SiO_2/Si$ substrate. The phase structure, converse piezoelectric coefficient and domain structure of $BaTiO_3$, $BiFeO_3$ and $BiFeO_3/BaTiO_3$ thin films are characterized by XRD and PFM, respectively. The converse piezoelectric coefficient d_{33} of $BiFeO_3/BaTiO_3$ thin films is 119.5 pm V^{-1}, which is comparable to that of lead-based piezoelectric films. The large piezoelectric response of $BiFeO_3/BaTiO_3$ thin films is ascribed to the low-symmetry T-like phase $BiFeO_3$, because the spontaneous polarization vector of T-like phase (with monoclinic symmetry) $BiFeO_3$ can rotate easily under external field. In addition, the reduced leakage current and major domains with upward polarization are also attributed to the large piezoelectricity.

1. Introduction

$BiFeO_3$ continues to reveal itself as one of the most intriguing materials.[1–3] Recently, studies have demonstrated that low-symmetry tetragonal- and rhombohedral-like (T- or R-like) phases can be easily triggered by mismatch stress in the epitaxial $BiFeO_3$ thin films.[4–6] Furthermore, *in situ* transmission electron microscopy has revealed that a large piezoelectric response can be obtained during the electric field- or pressure-induced phase transition from the T- or R-like phase to the pure T or R phase.[7] The low-symmetry phases are thought to be responsible for the large piezoelectric response, because the spontaneous polarization vector of the low symmetry phases can rotate within a monoclinic plane instead of lying along a symmetry axis as in the T and R phase structure.[8,9] Thus, $BiFeO_3$ is a promising lead-free candidate for the future piezoelectric applications.

However, due to the large leakage current, it is hard to obtain large piezoelectric response in $BiFeO_3$ polycrystalline films.[1,10] In the $BiFeO_3$ polycrystalline film deposited on the $Pt/TiO_2/SiO_2/Si$ substrate, the interfacial reaction between platinum and bismuth leads to abundant Bi deficiency.[11] As the Bi deficiency increased, a leakage current at $Pt/BiFeO_3$ interfaces tended to increase.[12] Generally, in order to enhance the property and reduce the leakage current of $BiFeO_3$ polycrystalline films, great efforts have been devoted to using Sm, La, Gd partially substituted at the Bi site in the $BiFeO_3$ polycrystalline film.[13,14] However, the study of the piezoelectricity, especially for the large piezoelectricity, of pure $BiFeO_3$ polycrystalline films is limited.

The leakage current of $BiFeO_3$ polycrystalline films can also be effectively reduced through introducing a buffer layer, because the buffer layer prevents the direct contact of $BiFeO_3$ and Pt.[15,16] In addition, enormous stresses are existed in the as-grown $BiFeO_3$ polycrystalline film[17] due to the differences in crystal lattice parameters and thermal expansion coefficients between the buffer layer and $BiFeO_3$ films, which may affect the phase structure and properties of the films. In the present study, a large piezoelectric response $BiFeO_3$ polycrystalline film with a $BaTiO_3$ buffer layer was prepared by the radio frequency magnetron sputtering. For comparison, $BiFeO_3$, $BaTiO_3$ polycrystalline films without buffer layers were also prepared *via* the same method. In addition, the effect of $BaTiO_3$ buffer layer and the mechanism of the large piezoelectric response were discussed.

2. Experimental

The $BaTiO_3$, $BiFeO_3$ and $BiFeO_3/BaTiO_3$ thin films were prepared by the radio frequency magnetron sputtering with the $BiFeO_3$ and $BaTiO_3$ target, respectively. Prior to the deposition, a base pressure of 5.0×10^{-4} Pa was achieved in the deposition chamber and the targets were pre-sputtered for 15 min to eliminate the surface heterogeneity. The $BaTiO_3$ thin film was

[a] *School of Materials Science and Engineering, Harbin Institute of Technology, Harbin 150001, People's Republic of China. E-mail: wdfei@hit.edu.cn; Fax: +86-451-86413908; Tel: +86-451-86413908*

[b] *National Key Laboratory of Science and Technology on Precision Heat Processing of Metals, Harbin Institute of Technology, Harbin 150001, People's Republic of China*

[c] *Department of Materials Science and Engineering, Harbin Institute of Technology Shenzhen Graduate School, Shenzhen 518055, P. R. China*

deposited on the Pt/Ti/SiO_2/Si substrate firstly, then the $BiFeO_3$ thin film was deposited on the $BaTiO_3$ thin film by the magnetron sputtering with an RF sputtering power of 40 W at 400 °C for 2 hours (each layer), under a mixed atmosphere of oxygen (0.3 Pa) and argon (0.9 Pa). For comparison, $BiFeO_3$ and $BaTiO_3$ monolayer films were also prepared under the same deposition conditions. Finally, the resulting films were annealed at 550 °C for 30 min. In addition, because the $BaTiO_3$ film was amorphous after 550 °C treatment, it was annealed at 750 °C again. The top platinum electrodes with a size of 3.14×10^{-4} cm^2 were deposited by the DC magnetron sputtering before piezoelectric response testing.

The XRD experiment was performed using an X'pert diffractometer using Cu Kα radiation at 40 kV and 40 mA, including the phase structure and stress analysis. The surface and cross-sectional morphologies of $BaTiO_3$, $BiFeO_3$ and $BiFeO_3$/$BaTiO_3$ thin films were observed by atomic force microscopy (CSPM5600 of Benyuan) and scanning electron microscopy (Helios Nanolab600i), respectively. The leakage behavior of $BiFeO_3$ and $BiFeO_3$/$BaTiO_3$ thin films was measured using a ferroelectric test system (P-LC100, Radiant Technology). The converse piezoelectric coefficients d_{33} of $BaTiO_3$, $BiFeO_3$ and $BiFeO_3$/$BaTiO_3$ thin films were characterized using a commercial scanning force microscope (CSPM5600 of Benyuan) equipped with a lock-in amplifier (model SR530, Standford Research System, Inc.). The input ac sine wave voltage, with amplitude in the range of 0–2 V and a frequency of 5 kHz, was applied between the conductive tip (top electrode) and the bottom electrode. The corresponding vertical deflection signal of the cantilever is recorded using a lock-in amplifier. Then the amplitude of the tip vibration was derived by multiplying the deflection signal with the calibration constant of the photodetector sensitivity. The domain structures of $BiFeO_3$/$BaTiO_3$, $BiFeO_3$ and $BaTiO_3$ thin films were characterised using the PFM image measurement (Brucker multimode 8) in the piezoelectric contact mode.

3. Results and discussion

The XRD patterns of $BaTiO_3$, $BiFeO_3$ and $BiFeO_3$/$BaTiO_3$ thin films are shown in Fig. 1.

As shown in Fig. 1(a), the $BaTiO_3$ film is amorphous after 550 °C treatment for 30 min. For comparison, the $BaTiO_3$ film is crystallized until 750 °C annealing treatment. Fig. 1(b) reveals that $BiFeO_3$ in both $BiFeO_3$ and $BiFeO_3$/$BaTiO_3$ thin films is well crystallized without detectable impurities or other phases. Only (010) reflections of $BiFeO_3$ can be clearly observed, so it can be concluded that the $BiFeO_3$ films are highly (010)-oriented. Moreover, it is observed from Fig. 1(b) that the profiles of (010) reflection of $BiFeO_3$ thin films are symmetric. In contrast, the profiles of (010) reflection of $BiFeO_3$/$BaTiO_3$ thin films are asymmetric.

To clearly analyze the difference between the (010) reflections of $BiFeO_3$ and $BiFeO_3$/$BaTiO_3$ thin films, fine scan XRD measurements were carried out. The measured and fitted profiles of (010) reflections (using pseudo-cubic coordinate system)

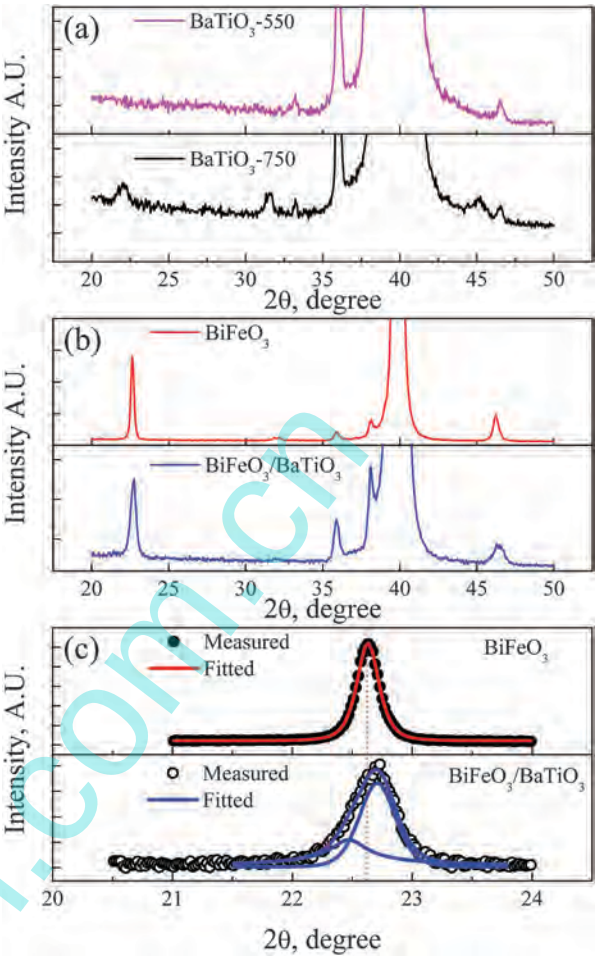

Fig. 1 (a) θ–2θ scan XRD patterns of $BaTiO_3$ thin films with 550 °C and 750 °C treatment, (b) $BiFeO_3$ and $BiFeO_3$/$BaTiO_3$ thin films with 550 °C treatment, (c) the measured and fitted profiles of (010) reflections of $BiFeO_3$ and $BiFeO_3$/$BaTiO_3$ thin films.

of $BiFeO_3$ and $BiFeO_3$/$BaTiO_3$ thin films are shown in Fig. 1(c). For the R phase of $BiFeO_3$ (*R3m* space group), it is well established that the profile of (010) reflection is singlet, whereas the profiles of (010) reflections for the T-like phase are doublet.[18] Following this, the phase structure of $BiFeO_3$ thin films is R, because the (010) reflection is a symmetry singlet as shown in Fig. 1(c). However, an asymmetric (010) reflection of $BiFeO_3$/$BaTiO_3$ thin films indicates clearly the (010) peak splitting. The splitting of the (010) peak means that the phase structure of $BiFeO_3$/$BaTiO_3$ thin films is not R anymore, but a phase transition has taken place. According to previous reports,[1,8,16] the T-like phase can be induced by the strain in $BiFeO_3$ films. In the present study, we consider that the phase structure of $BiFeO_3$/$BaTiO_3$ thin films might be the T-like phase. Thus it is suggested that the phase structure of $BiFeO_3$/$BaTiO_3$ thin films undergoes a change from the R to T-like phase.

Fig. 2 shows the surface and cross-section micrographs of $BaTiO_3$, $BiFeO_3$ and $BiFeO_3$/$BaTiO_3$ thin films. From the surface micrographs (Fig. 2a, c and e), it can be seen that both $BaTiO_3$ and $BiFeO_3$/$BaTiO_3$ thin films consist of nanoparticles with small surface roughness, while the surface of $BiFeO_3$ films is inhomogenous. The cross-section micrographs of $BaTiO_3$, $BiFeO_3$

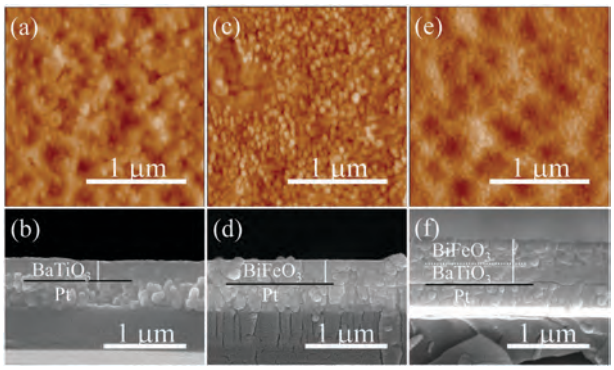

Fig. 2 The surface and cross-section micrographs of (a) and (b) $BaTiO_3$ thin films, (c) and (d) $BiFeO_3$ thin films, (e) and (f) $BiFeO_3/BaTiO_3$ thin films.

and $BiFeO_3/BaTiO_3$ thin films are shown in Fig. 2(b), (d) and (f), respectively. From the SEM results, it can be seen that the thicknesses of the $BaTiO_3$, $BiFeO_3$ and $BiFeO_3/BaTiO_3$ thin films are 240 nm, 270 nm and 535 nm, respectively. It is worth noting that in the $BiFeO_3$ thin film, particles are throughout the entire film ($BiFeO_3$ and Pt) and the interface between $BiFeO_3$ and Pt films is obscure. The obscure interface between $BiFeO_3$ and Pt films and the imhomogenous surface of $BiFeO_3$ films may be caused by the interface reaction between platinum and bismuth.[11] Thus, the stress in the $BiFeO_3$ polycrystalline film is relaxed. However, in the $BiFeO_3/BaTiO_3$ thin film, the interface between $BiFeO_3$ and $BaTiO_3$ films is clearly distinguished, which indicates a large stress in the $BiFeO_3$ polycrystalline film. The large stress may be the reason for the presence of a T-like phase, which is in accordance with the XRD results.

The dielectric properties of $BaTiO_3$, $BiFeO_3$ and $BiFeO_3/BaTiO_3$ polycrystalline films were measured at room temperature as a function of frequency ranging from 500 Hz to 1 MHz and the results are given in Fig. 3(a) and (b). From Fig. 3(a), it can be observed that the dielectric constants of $BaTiO_3$, $BiFeO_3$ and $BiFeO_3/BaTiO_3$ polycrystalline films are 200, 100 and 50 at a frequency of 1 kHz, respectively. The small dielectric constant of $BiFeO_3/BaTiO_3$ polycrystalline films is caused by the parallel-connect $BiFeO_3$ and amorphous $BaTiO_3$ film. More importantly, as shown in Fig. 3(b), the dielectric loss of $BiFeO_3/BaTiO_3$ polycrystalline films is much lower than that of $BaTiO_3$ and $BiFeO_3$ films at a frequency ranging from 500 kHz to 1 MHz, especially for the high frequency. To assess the leakage behavior, the leakage current density (J) *versus* the electric field (E) curves of $BiFeO_3$ and $BiFeO_3/BaTiO_3$ polycrystalline films are shown in Fig. 3(c). From Fig. 3(c), it is observed that the $BiFeO_3$ polycrystalline film exhibits high leakage current density, while the $BiFeO_3/BaTiO_3$ polycrystalline film shows greatly reduced leakage current density. The reduced dielectric loss and leakage current is caused by the following reasons: firstly, $BaTiO_3$ buffer layers prevent the interface reaction between Bi and Pt, which reduces the Bi deficiency; secondly, $BaTiO_3$ is a good insulator, which is helpful to enhance the electrical resistivity of $BiFeO_3/BaTiO_3$ polycrystalline films.

Fig. 3(d) shows the ferroelectric polarization *versus* electric field curves (P–E hysteresis loops) of the $BaTiO_3$, $BiFeO_3$ and

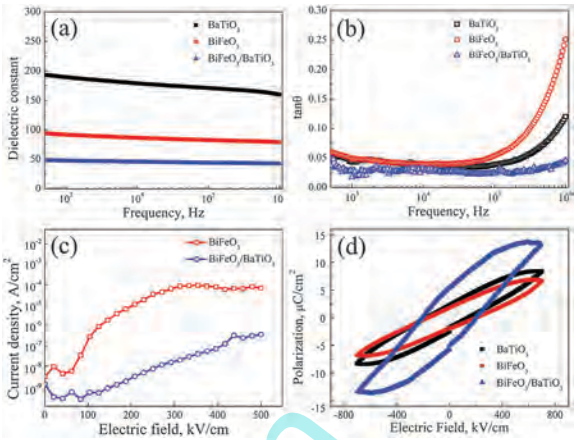

Fig. 3 Electric proprieties of $BaTiO_3$, $BiFeO_3$ and $BiFeO_3/BaTiO_3$ polycrystalline films, (a) frequency dependence of dielectric permittivity, (b) frequency dependence of dielectric loss, (c) J–E curves, (d) P–E hysteresis loops.

$BiFeO_3/BaTiO_3$ polycrystalline films measured at 1 kHz. It can be seen that the remnant polarization (P_r) of $BiFeO_3/BaTiO_3$ polycrystalline films is nearly twice as large as that of $BaTiO_3$ and $BiFeO_3$ films. The greatly enhanced ferroelectricity and electrical resistivity mean that the $BiFeO_3/BaTiO_3$ film can be polarized under higher electric bias and exhibit higher remnant polarization.

Taking the T-like phase, reduced leakage current and easy to polarization of the $BiFeO_3/BaTiO_3$ polycrystalline film into consideration, a large piezoelectric response of $BiFeO_3/BaTiO_3$ thin films is expected. The converse piezoelectric coefficients (d_{33}) of $BaTiO_3$, $BiFeO_3$ and $BiFeO_3/BaTiO_3$ thin films were characterized using a commercial scanning force microscope equipped with a lock-in amplifier (for detailed information please see the experiment part).[19] The measured and linear fitted results are shown in Fig. 4(a), and the slope of the fitted line represents d_{33} of the samples.[20,21] It can be seen that d_{33} of $BaTiO_3$ thin films is 67.1 pm V^{-1} (k_1 shown in Fig. 4a), which is consistent with the other previous studies.[22] The d_{33} value of $BiFeO_3/BaTiO_3$ polycrystalline films is 119.5 pm V^{-1} (k_3 shown in Fig. 4a), which is comparable with that of the lead-based piezoelectric films. While the d_{33} value of $BiFeO_3$ thin films is only 32.8 pm V^{-1} (k_2 shown in Fig. 4a). It is well known that the

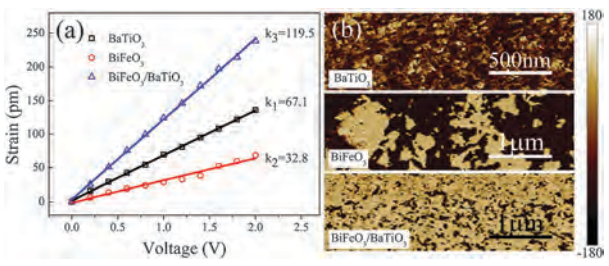

Fig. 4 Converse piezoelectric coefficient (d_{33}) and domain structures of $BaTiO_3$, $BiFeO_3$ and $BiFeO_3/BaTiO_3$ polycrystalline films, (a) measured and linearly fitted experimental data for d_{33}, (b) domain structures of $BaTiO_3$, $BiFeO_3$ and $BiFeO_3/BaTiO_3$ polycrystalline films.

large piezoelectric response is related to the ease of phase transition or polarization rotation under external stimuli.[4] In this study, a low-symmetry T-like phase is found in the $BiFeO_3$/$BaTiO_3$ thin film. The T-like phase is regarded as a structure bridge between the R and T phase,[23] thus in this case R–T phase transition is more easy through the T-like phase, which may be helpful for the excellent piezoelectric performance. Furthermore, the polarization vector of the T-like phase can be rotated within a monoclinic plane.[8,9,24,25] Thus in the $BiFeO_3$/$BaTiO_3$ polycrystalline film, the ease of polarization rotation of the T-like phase under external stimuli may also lead to a large piezoelectric response. This similar result has been reported in the lead-based system.[24] In addition, $BiFeO_3$ in the $BiFeO_3$/$BaTiO_3$ polycrystalline film can be fully polarized due to the reduced leakage current density, which is also helpful to the large piezoelectric response of the $BiFeO_3$/$BaTiO_3$ polycrystalline film.

To further understand the mechanism of large response of $BiFeO_3$/$BaTiO_3$ polycrystalline films on the domain scale, out-of-plane domain structures (upward or downward) of $BaTiO_3$, $BiFeO_3$ and $BiFeO_3$/$BaTiO_3$ polycrystalline films were characterised using PFM. The test results are shown in Fig. 4(b), and the brightness difference in Fig. 4(b) means the domain with different directions of polarization. As shown in the top image of Fig. 4(b), the $BaTiO_3$ thin film consists of many small domain structures with different polarization, which may be the reason for the good piezoelectricity of $BaTiO_3$ thin films. In the middle image of Fig. 4(b), it is observed that there are many large domains with upward or downward polarization in the $BiFeO_3$ thin film. Furthermore, the large leakage current of $BiFeO_3$ thin films prevents the sample to fully polarize, thus the piezoelectricity of $BiFeO_3$ thin films is poor. As shown in the bottom image in Fig. 4(b), in contrast to the domain structure of $BiFeO_3$ thin films, the major domain regions are upward polarized in $BiFeO_3$/$BaTiO_3$ thin films and the polarization vector of these domain region is easily polarized in the out-of-plane direction (perpendicular to substrates) under external stimuli, which may be helpful to the large piezoelectric response of $BiFeO_3$/$BaTiO_3$ thin films. In addition, the self-polarization is also contributed to the large piezoelectric response of $BiFeO_3$/$BaTiO_3$ polycrystalline films.[26]

4. Conclusions

In this work, $BaTiO_3$, $BiFeO_3$ and $BiFeO_3$/$BaTiO_3$ polycrystalline films were prepared by the radio frequency magnetron sputtering on the Pt/Ti/SiO_2/Si substrate. The phase structure, converse piezoelectric coefficient (d_{33}) and domain structure of $BaTiO_3$, $BiFeO_3$ and $BiFeO_3$/$BaTiO_3$ thin films are characterized by XRD and PFM, respectively. In the $BiFeO_3$/$BaTiO_3$ polycrystalline film, due to the stress supplied by the bottom $BaTiO_3$ thin film, the phase structure of $BiFeO_3$ is the T-like phase, which is different from that of pure $BiFeO_3$ thin films (R phase). Furthermore, $BiFeO_3$/$BaTiO_3$ thin films show greatly reduced leakage current density. Because of the existed low-symmetry T-like phase, reduced leakage current density, and major domains with upward polarization, $BiFeO_3$/$BaTiO_3$ thin films exhibit excellent piezoelectricity with a d_{33} value of 119.5 pm V^{-1}, which is comparable to that of lead-based piezoelectric films.

Acknowledgements

The research was financially supported by the National Natural Science Foundation of China (No. 11272102) and Research Foundation of Shenzhen Science, Technology and Innovation Commission (No. JCYJ20120613133835232).

Notes and references

1 J. Wang, J. B. Neaton, H. Zheng, V. Nagarajan, S. B. Ogale, D. V. B. Liu, V. Vaithyanathan, D. G. Schlom, N. A. S. U. V. Waghmare, K. M. Rabe and R. R. M. Wuttig, *Science*, 2003, **299**, 1719–1722.
2 S. Xie, A. Gannepalli, Q. N. Chen, Y. Liu, Y. Zhou, R. Proksch and J. Li, *Nanoscale*, 2012, **4**, 408–413.
3 N. M. Aimon, D. Hun Kim, H. Kyoon Choi and C. A. Ross, *Appl. Phys. Lett.*, 2012, **100**, 092901.
4 Z. Chen, S. Prosandeev, Z. L. Luo, W. Ren, Y. Qi, C. W. Huang, L. You, C. Gao, I. A. Kornev, T. Wu, J. Wang, P. Yang, T. Sritharan, L. Bellaiche and L. Chen, *Phys. Rev. B: Condens. Matter Mater. Phys.*, 2011, **84**, 094116.
5 Z. Chen, Z. Luo, Y. Qi, P. Yang, S. Wu, C. Huang, T. Wu, J. Wang, C. Gao, T. Sritharan and L. Chen, *Appl. Phys. Lett.*, 2010, **97**, 242903.
6 S. H. B. H. W. Jang, D. Ortiz, C. M. Folkman, R. R. Das, Y. H. Chu, P. Shafer, J. X. Zhang, S. Choudhury, Y. B. C. V. Vaithyanathan, D. A. Felker, M. D. Biegalski, M. S. Rzchowski, X. Q. Pan, D. G. Schlom, R. R. L. Q. Chen and C. B. Eom, *Phys. Rev. Lett.*, 2008, **101**, 107602.
7 B. X. J. X. Zhang, Q. He, J. Seidel, R. J. Zeches, P. Yu, S. Y. Yang, C. H. Wang, Y. H. Chu and A. M. M. a. R. R. L. W. Martin, *Nat. Nanotechnol.*, 2011, **6**, 98–102.
8 Z. Wu and R. Cohen, *Phys. Rev. Lett.*, 2005, **95**, 037601.
9 M. D. Nguyen, M. Dekkers, E. Houwman, R. Steenwelle, X. Wan, A. Roelofs, T. Schmitz-Kempen and G. Rijnders, *Appl. Phys. Lett.*, 2011, **99**, 252904.
10 S. O. Leontsev and R. E. Eitel, *J. Mater. Res.*, 2011, **26**, 9–17.
11 J. K. Kim, S. S. Kim, M. H. Park, J. W. Kim, E. J. Choi, T. G. Ha, H. K. Cho, R. Guo and A. S. Bhalla, *Ferroelectrics*, 2007, **350**, 118–123.
12 A. Tsurumaki, H. Yamada and A. Sawa, *Adv. Funct. Mater.*, 2012, **22**, 1040–1047.
13 F. Yan, T. J. Zhu, M. O. Lai and L. Lu, *Scr. Mater.*, 2010, **63**, 780–783.
14 S. Fujino, M. Murakami, V. Anbusathaiah, S. H. Lim, V. Nagarajan, C. J. Fennie, M. Wuttig, L. Salamanca-Riba and I. Takeuchi, *Appl. Phys. Lett.*, 2008, **92**, 202904.
15 F. Huang, X. Lu, W. Lin, W. Cai, X. Wu, Y. Kan, H. Sang and J. Zhu, *Appl. Phys. Lett.*, 2007, **90**, 252903.
16 D. H. Wang, L. Yan, C. K. Ong and Y. W. Du, *Appl. Phys. Lett.*, 2006, **89**, 182905.

17 K. J. Choi, M. Biegalski, Y. L. Li, A. Sharan, J. Schubert, P. R. R. Uecker, Y. B. Chen, X. Q. Pan, V. Gopalan, D. G. S. L.-Q. Chen and C. B. Eom, *Science*, 2004, **306**, 1005–1009.
18 S. Q. Zhang, L. D. Wang, W. L. Li, N. Li and W. D. Fei, *J. Alloys Compd.*, 2011, **509**, 2976–2980.
19 T. D. Z. W. L. Li, Y. F. Hou, Y. Zhao, D. Xu, W. P. Cao and W. D. Fei, *RSC Adv.*, 2014, **4**, 56933–56937.
20 A. G. Agronin, Y. Rosenwaks and G. I. Rosenman, *Nano Lett.*, 2003, **3**, 169–171.
21 M. H. Zhao, Z. L. Wang and S. X. Mao, *Nano Lett.*, 2004, **4**, 587–590.
22 I. D. Kim, Y. Avrahami, H. L. Tuller, Y.-B. Park, M. J. Dicken and H. A. Atwater, *Appl. Phys. Lett.*, 2005, **86**, 192907.
23 Z. Chen, Z. Luo, C. Huang, Y. Qi, P. Yang, L. You, C. Hu, T. Wu, J. Wang, C. Gao, T. Sritharan and L. Chen, *Adv. Funct. Mater.*, 2011, **21**, 133–138.
24 B. Noheda, D. E. Cox, G. Shirane, S. E. Park, L. E. Cross and Z. Zhong, *Phys. Rev. Lett.*, 2001, **86**, 3891–3894.
25 D. Vanderbilt and M. Cohen, *Phys. Rev. B: Condens. Matter Mater. Phys.*, 2001, **63**, 094108.
26 X. Chen, Y. Zou, G. Yuan, M. Zeng, J. M. Liu, J. Yin, Z. Liu and X. M. Chen, *J. Am. Ceram. Soc.*, 2013, **96**, 3788–3792.